BMC Pediatrics

RESEARCH

Open Access

Image-based deep learning in diagnosing mycoplasma pneumonia on pediatric chest X-rays

Xing-hao Lan[1†], Yun-xu Zhang[2†], Wei-hua Yuan[3*], Fei Shi[2*] and Wan-liang Guo[1*]

Abstract

Background Correctly diagnosing and accurately distinguishing mycoplasma pneumonia in children has consistently posed a challenge in clinical practice, as it can directly impact the prognosis of affected children. To address this issue, we analyzed chest X-rays (CXR) using various deep learning models to diagnose pediatric mycoplasma pneumonia.

Methods We collected 578 cases of children with mycoplasma infection and 191 cases of children with virus infection, with available CXR sets. Three deep convolutional neural networks (ResNet50, DenseNet121, and EfficientNetv2-S) were used to distinguish mycoplasma pneumonia from viral pneumonia based on CXR. Accuracy, area under the curve (AUC), sensitivity, and specificity were used to evaluate the performance of the model. Visualization was also achieved through the use of Class Activation Mapping (CAM), providing more transparent and interpretable classification results.

Results Of the three models evaluated, ResNet50 outperformed the others. Pretrained with the ZhangLabData dataset, the ResNet50 model achieved 80.00% accuracy in the validation set. The model also showed robustness in two test sets, with accuracy of 82.65 and 83.27%, and AUC values of 0.822 and 0.758. In the test results using ImageNet pre-training weights, the accuracy of the ResNet50 model in the validation set was 80.00%; the accuracy in the two test sets was 81.63 and 62.91%; and the corresponding AUC values were 0.851 and 0.776. The sensitivity values were 0.884 and 0.595, and the specificity values were 0.655 and 0.814.

Conclusions This study demonstrates that deep convolutional networks utilizing transfer learning are effective in detecting mycoplasma pneumonia based on chest X-rays (CXR). This suggests that, in the near future, such computer-aided detection approaches can be employed for the early screening of pneumonia pathogens. This has

†Xing-hao Lan and Yun-xu Zhang contributed equally to this work.

*Correspondence:
Wei-hua Yuan
19362278@qq.com
Fei Shi
shifei@suda.edu.cn
Wan-liang Guo
gwlsuzhou@163.com

Full list of author information is available at the end of the article

© The Author(s) 2024. **Open Access** This article is licensed under a Creative Commons Attribution-NonCommercial-NoDerivatives 4.0 International License, which permits any non-commercial use, sharing, distribution and reproduction in any medium or format, as long as you give appropriate credit to the original author(s) and the source, provide a link to the Creative Commons licence, and indicate if you modified the licensed material. You do not have permission under this licence to share adapted material derived from this article or parts of it. The images or other third party material in this article are included in the article's Creative Commons licence, unless indicated otherwise in a credit line to the material. If material is not included in the article's Creative Commons licence and your intended use is not permitted by statutory regulation or exceeds the permitted use, you will need to obtain permission directly from the copyright holder. To view a copy of this licence, visit http://creativecommons.org/licenses/by-nc-nd/4.0/.

significant clinical implications for the rapid diagnosis and appropriate medical intervention of pneumonia, potentially enhancing the prognosis for affected children.

Keywords Mycoplasma pneumoniae, Pneumonia, Deep learning, X-ray, Pediatric

Introduction

Mycoplasma pneumoniae (*M. pneumoniae*) is an important infectious pathogen of the lower respiratory tract. The pathogen is transmitted via respiratory droplets, and people are usually infected after close contact with patients with symptomatic infection [1]. *M. pneumoniae* pneumonia (MPP) is often considered a self-limited disease, but the development of refractory MPP (RMPP) is possible, which usually worsens after 7 days or more of conventional macrolide antibiotic treatment [2, 3]. RMPP can lead to a variety of pulmonary and extrapulmonary complications [4], which in some cases can progress to necrotizing pneumonia [5]. In the years following COVID-19, there has been a significant increase in the number of respiratory infections in children due to the so-called "immunization debt," which is not fully consistent with previous seasonality [6, 7]. Especially in the autumn and winter of 2023, there were a large number of children with mycoplasma infection all over China, significantly more than in previous years. Among them there were considerable number of severe cases, which caused great harm to the body and mind of the children and increased the burden on the families. Therefore, rapid and accurate diagnosis plays a crucial role in the treatment of mycoplasma pneumonia and the good prognosis of children.

Chest X-ray (CXR) imaging as a rapid, low-cost, and noninvasive examination method with low radiation exposure, plays an important role in the assessment of pulmonary disease, especially in the diagnosis and treatment of respiratory infections in children. However, it is difficult to make a diagnosis of etiology only by looking at CXR with the naked eye.

Deep learning is a machine-learning technique in artificial intelligence (AI) technology that uses artificial neural networks as computational models to discover complex structures and patterns in large high-dimensional datasets [8]. There have been an increasing number of studies describing the application of deep learning in medical imaging fields, including CXR imaging [9]. Given their availability and abundance, CXR images are particularly suitable for analysis using computer-based techniques ranging from traditional machine learning and pattern recognition to emerging deep convolutional neural networks [10, 11].

Currently, deep learning methods that utilize CXR images have been extensively applied in medical research, as demonstrated in studies by Prathiksha et al. [12] and Enes et al. [13]. Their research primarily emphasized the enhancement of early and accurate diagnoses of pneumonia. However, these studies did not extend to the analysis of specific pathogens responsible for pneumonia, particularly in pediatric patients. Differentiation of mycoplasma pneumonia and viral pneumonia in children is still a challenge in clinical practice. Therefore, we investigated the application of deep learning in the detection of mycoplasma pneumonia. The aim was to provide an accurate binary classification (mycoplasma pneumonia vs. viral pneumonia) and to provide an earlier and faster diagnosis for clinical treatment in the future.

Patients and methods

We collected 578 children with mycoplasma infection and 191 children with viral infection, ranging in age from 1 month to 15 years. The pathogens were confirmed by molecular biological methods (polymerase chain reaction, PCR) on sputum samples collected from the Children's Hospital of Soochow University and Changzhou Children's Hospital during August and September 2023. The CXR images of these children were characterized and analyzed by deep learning using convolution neural network (CNN) models of three different structures and two different sets of pre-training weights.

Data acquisition

Two pneumonia datasets were collected, namely one from the Children's Hospital of Soochow University, which included 494 patients (148 cases of viral pneumonia and 346 cases of mycoplasma pneumonia), and the other from the Changzhou Children's Hospital, which included 275 patients (43 cases of viral pneumonia and 232 cases of mycoplasma pneumonia). All data were de-identified. The pediatric pneumonia datasets were exempted from review by the institutional review board of the Children's Hospital of Soochow University and Changzhou Children's Hospital. As this was a retrospective study, informed consent from each subject was exempted by the institutional review board of the Children's Hospital of Soochow University and Changzhou Children's Hospital.

Data preprocessing

The raw CXR data were in DICOM format and were converted to JPG image format using Python (3.11.5). This format is not only easier to operate but is also a commonly used data format for deep learning and does not decrease the image fidelity. Due to the inconsistency in dynamic range of the intensity between the two datasets

in our study (one was 8-bit and the other was 16-bit), the image intensity was normalized to a range of −1024 to 1024 during read-in. This was followed by histogram equalization to reduce the differences in contrast and improve the generalization performance of the model.

The images were center cropped to have the same number of rows and columns. Then the resolution of the images was further adjusted to 224×224 for network input. During training, data augmentation was performed, which included random rotation (within −15 to +15 degrees) and scaling (scaling factor between 0.5 and 1.5).

The Suzhou dataset was randomly split into the training (296 patients, including 89 cases of viral pneumonia and 207 cases of mycoplasma pneumonia), validation (100 patients, including 30 cases of viral pneumonia and 70 cases of mycoplasma pneumonia), and test (98 patients, including 29 cases of viral pneumonia and 69 cases of mycoplasma pneumonia) sets in a 60:20:20% ratio. The Changzhou dataset was treated as the second test set. The patients with viral pneumonia were defined as the negative group, while those with mycoplasma pneumonia were defined as the positive group.

Model implementation

In our study, three deep convolutional neural networks (ResNet50 [14], DenseNet121 [15], and EfficientNetv2-S [16]) were used to classify CXR images to determine whether there was mycoplasma pneumonia infection. The ResNet50 is a variant of the ResNet model, which is known for its skip connections that mitigate the vanishing gradient problem, thereby enabling the training of very deep networks. The DenseNet121 belongs to the family of Dense Convolutional Networks and is characterized by its dense connectivity pattern, connecting each layer to every other layer in a feed-forward fashion. This design promotes feature reuse, reduces the number of parameters, and enhances feature propagation throughout the network. The EfficientNetv2-S is part of the EfficientNetv2 family, which is designed to achieve better accuracy and efficiency compared with previous CNN architectures. The EfficientNetv2-S model uses a compound scaling method to balance network depth, width, and resolution, resulting in improved performance with fewer parameters. The cross-entropy was used as loss function for all networks.

An open-source machine-learning library, PyTorch, was used to implement the model. We used the following set of hyper-parameters: batchsize=16, learning rate=10^{-4}, epochs=100, and optimizers=adam. To address the issue of limited data, we employed transfer learning techniques. Transfer learning involves the utilization of pre-trained models obtained on large datasets, which are then fine-tuned on smaller, domain-specific datasets. This approach allowed us to leverage the knowledge and features acquired from the larger dataset, thereby enhancing the performance of our model on limited data. We utilized the CXR data from the ZhangLabData dataset [17], which comprised a total of 5856 X-ray images from children. Within this dataset, 2780 images were labeled as bacterial pneumonia, 1493 images were labeled as viral pneumonia, and the remaining images were labeled as normal. During the pre-training phase, we used the following set of hyper-parameters: batchsize=16, learning rate=3×10^{-4}, epochs=500, and optimizers=adam.

To provide more transparent and interpretable classification results, we conducted a qualitative analysis showing the areas that our model pays attention to. This was achieved through the use of Class Activation Mapping (CAM) [18], a technique that leverages feature visualization to delve into the inner workings and decision-making processes of deep convolutional neural networks. CAM produced a class activation map, essentially a grayscale image that emphasized the regions within an input image that were pivotal for the prediction of a specific class. To obtain CAM, the feature maps of the last convolutional layer of the network were globally average-pooled and then weighted by the learned weights of the fully connected layer. The resulting weighted feature maps were then summed to obtain the class activation map. The flowchart of this study is shown in Fig. 1.

Results

We selected the model that demonstrated the best performance in the validation set during the training phase. Figure 2 provides a comprehensive demonstration of the performance metrics during the training phase of the ResNet50 network. The graphical representations in Fig. 2(a) and 2(c) illustrate the model's accuracy in the training and validation sets, respectively, both of which exhibited an upward trend as the number of iterations increased. Figure 2(b) and 2(d) display the cross-entropy loss for the training and validation sets, respectively, serving as an indicator of the difference between the model's predictions and the actual values. Both of them were decreasing with iterations. It can be observed that, after 60 epochs of training, the models no longer showed significant improvement in accuracy or cross-entropy loss.

As shown in Table 1, among the three models evaluated, the ResNet50 outperformed the others, achieving an accuracy of 80.00% in the validation set. This model also demonstrated robust performance in the two test sets, with accuracy of 82.65 and 83.27%, and AUC values of 0.822 and 0.758(Fig. 3). The DenseNet121 model, while achieving a slightly higher accuracy of 81.00% in the validation set, fell short in the test sets with accuracy of 77.55

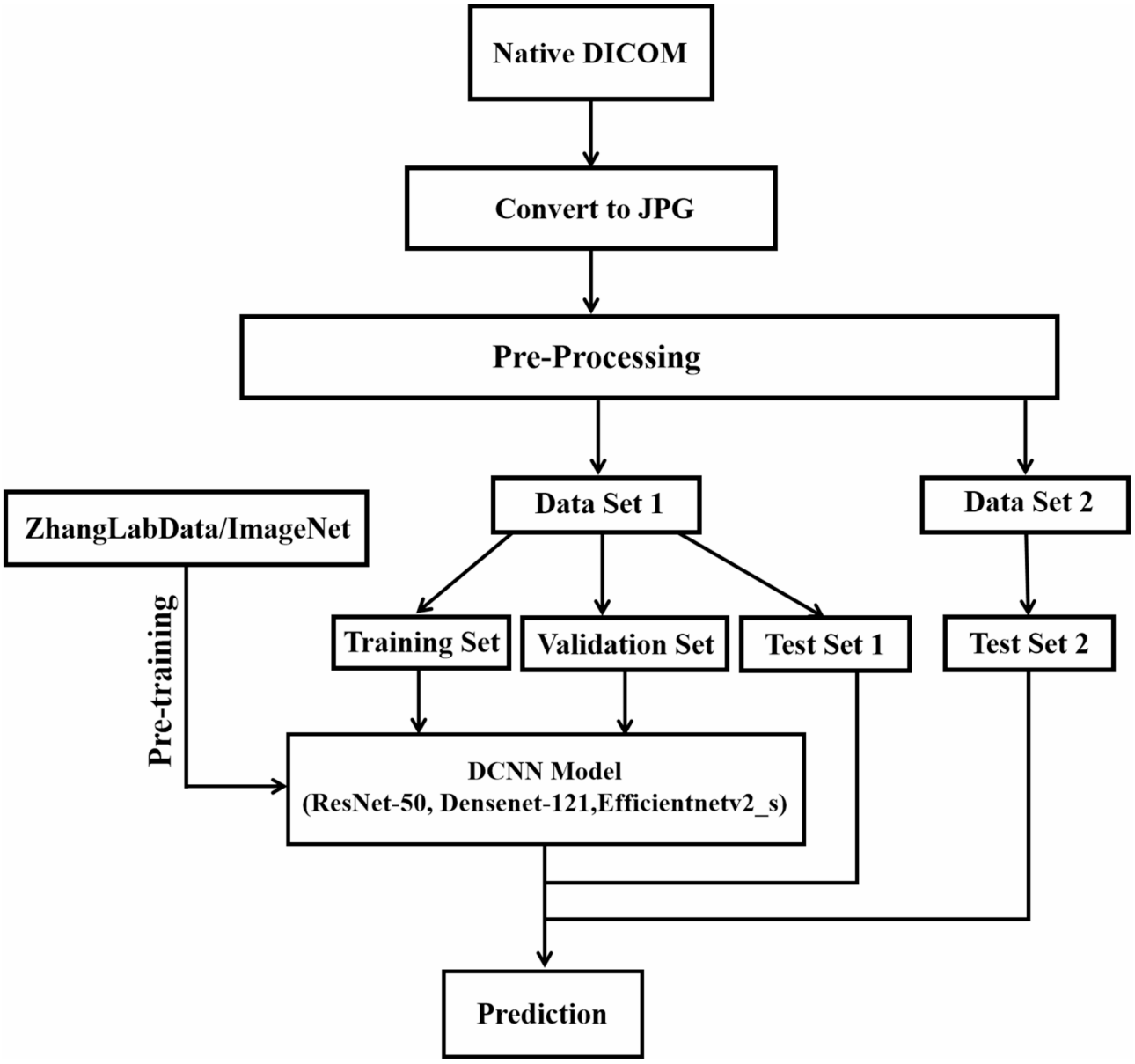

Fig. 1 Data flow diagram of using deep learning models for classification of mycoplasma pneumonia on two datasets. DICOM = digital imaging and communications in medicine; JPG = joint photographic experts group file format; DCNN = deep convolution neural networks

and 78.91%, and AUC values of 0.799 and 0.736. Lastly, the EfficientNetv2-S model matched the validation set accuracy of the ResNet50 model at 80.00%, but its performance in the test sets was lower, with accuracy of 74.49 and 79.64%, and AUC values of 0.823 and 0.767. The confusion matrices of ResNet50 obtained on the two test sets are shown in Fig. 4. The number of true positives for mycoplasma pneumonia detection is big, corresponding to the high sensitivity values in Table 2. To elucidate the impact of our pre-training methodology, we conducted a series of comparative experiments. These experiments employed identical model architectures, but differed in their initialization, which was carried out using the official ImageNet weights provided by PyTorch. As shown in Table 2, the ResNet50 model achieved an accuracy of 80.00% in the validation set, and 81.63 and 62.91% in the two test sets, with corresponding AUC values of 0.851 and 0.776, sensitivity values of 0.884 and 0.595, and specificity values of 0.655 and 0.814. The DenseNet 121 model displayed an accuracy of 81.00% in the validation set, and 71.00 and 74.45% in the two test sets, with AUC values of 0.792 and 0.780, sensitivity values of 0.928 and 0.733, and specificity values of 0.345 and 0.814. The EfficientNetv2-S model achieved an accuracy of 82.00% in the validation set, and 82.65% and 71.64% in the two test sets, with AUC values of 0.844 and 0.720, sensitivity

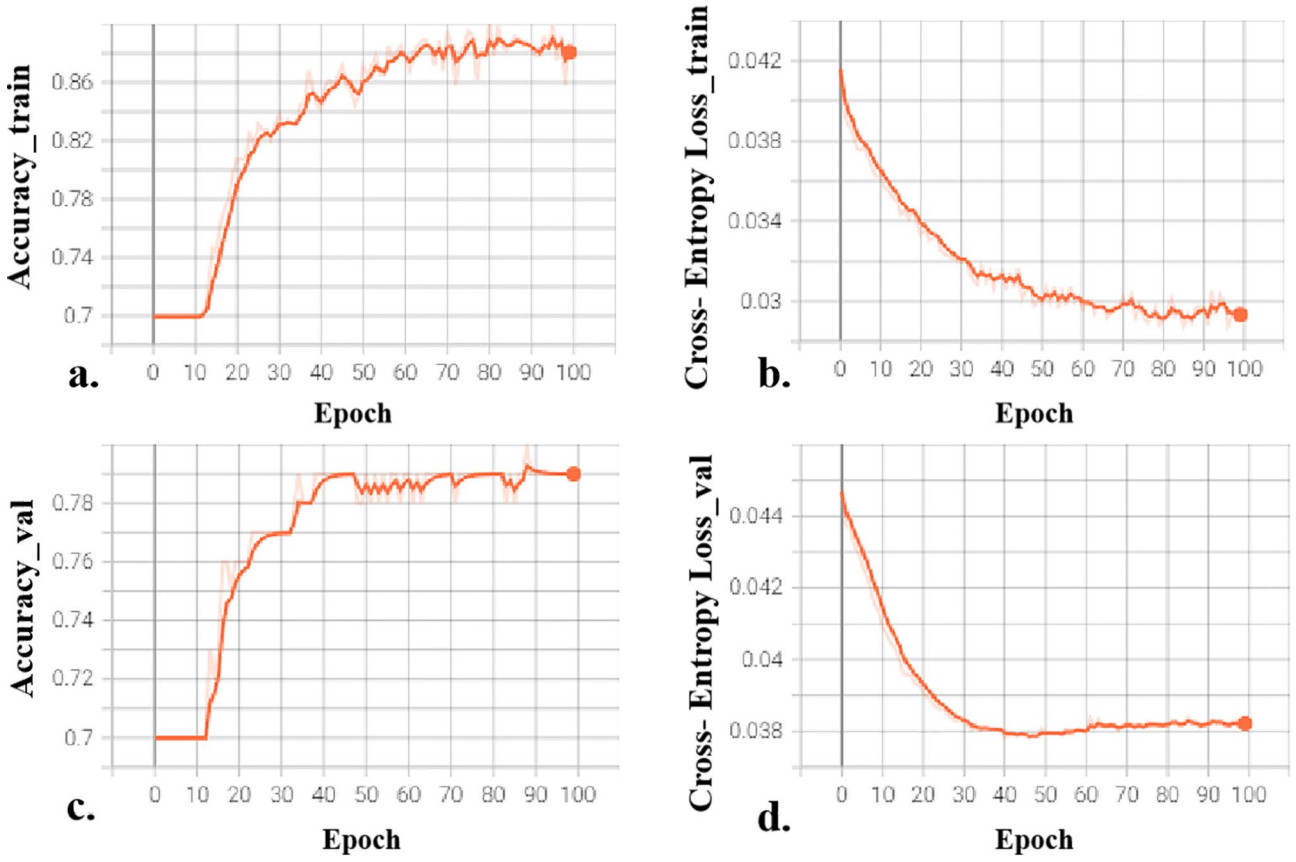

Fig. 2 Plot illustrates the accuracy and loss curves during the training of the Resnet50 model using Tensor board. (**a**, **b**) The accuracy and cross-entropy loss plotted on the training data, respectively. (**b**, **d**) The accuracy and cross-entropy loss plotted on the validation data, respectively. Plots were smoothed with a smoothing factor of 0.6 in order to clearly show the trend. train = training. val = validation

Table 1 Performance indices obtained by training using pre-training weights on the ZhangLabData dataset

	Number of Images		Resnet50	Densenet121	Efficientnetv2-s
validation	30VP/70 MP	Acc	80.00%	81.00%	80.00%
Test1	29VP/69MP	Acc	82.65%	77.55%	74.49%
		Auc	0.822	0.799	0.823
		Sen	0.971	0.928	0.855
		Spe	0.483	0.414	0.483
Test2	43VP/232MP	Acc	83.27%	78.91%	79.64%
		Auc	0.758	0.736	0.767
		Sen	0.884	0.845	0.828
		Spe	0.558	0.488	0.628

Acc: accuracy, Auc: Area Under the Curve, Sen: sensitivity, Spe: specificity

VP: viral pneumonia; MP: mycoplasma pneumonia

values of 0.957 and 0.754, and specificity values of 0.517 and 0.512.

To demonstrate the necessity of image pre-processing and data augmentation, we conducted some experiments in which histogram equalization and/or data augmentation were not applied. Table 3 shows that, when one or both of them are omitted, the overall performance become worse for both test sets. This indicates that these processing steps contribute to the generalization of the deep learning model.

Discussion

The clinical manifestations of MPP in children are not typical, and early diagnosis is easily missed [19]. Clinicians should make reasonable use of detection methods to achieve early and accurate diagnosis. At present, the conventional methods for the diagnosis of mycoplasma

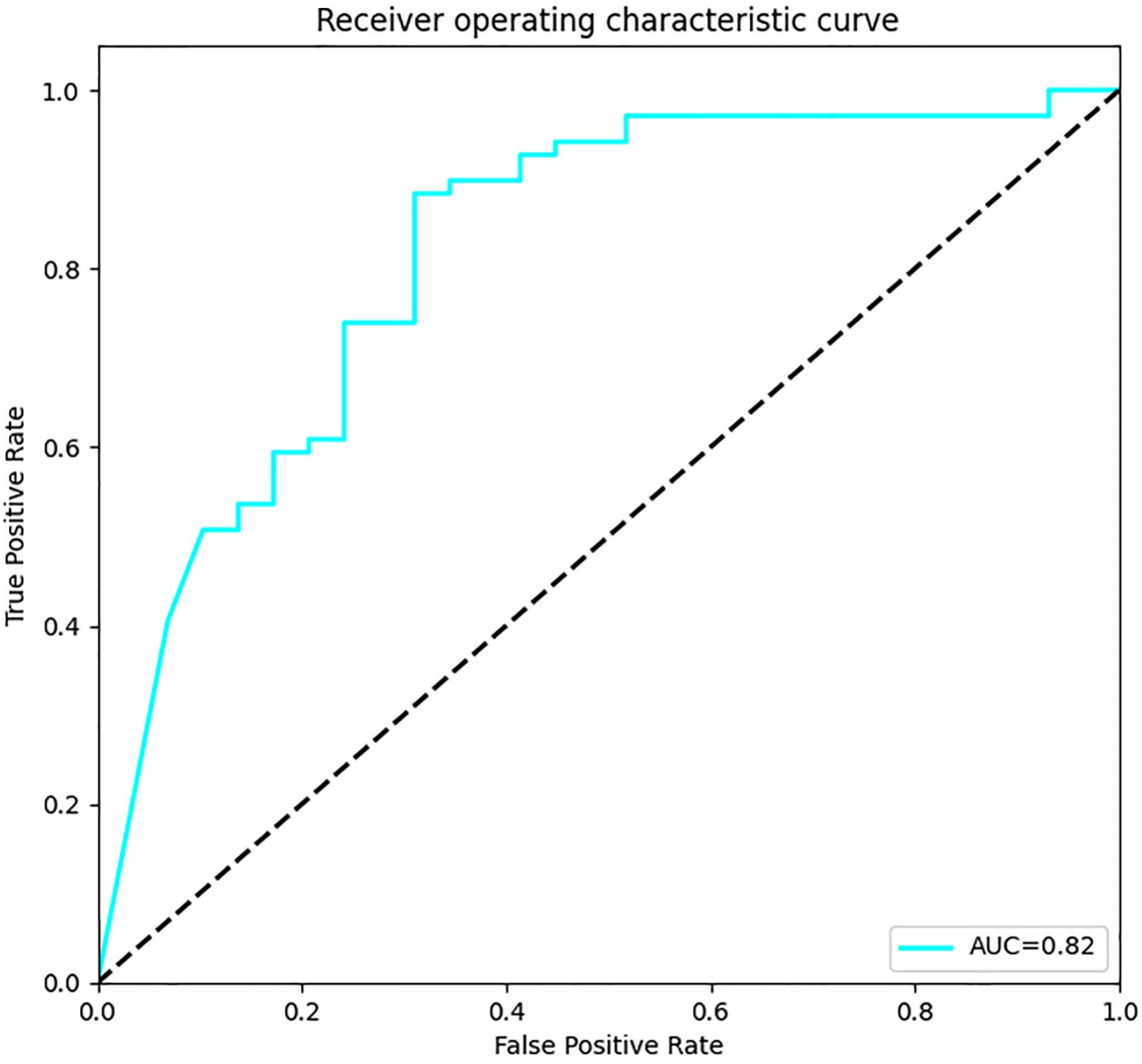

Fig. 3 The ROC curve for diagnosing whether a child has mycoplasma pneumonia on Test Set 1 using the ResNet50 model, whose AUC was 0.822

pneumonia are culture, nucleic acid detection, and antigen detection, but they either lack sufficient precision and accuracy, or are slow and expensive, which may delay the treatment, especially in the rapidly developing stage of childhood pneumonia [20, 21]. In this study, we used different deep-learning models to distinguish pediatric mycoplasma pneumonia from viral pneumonia on CXR, so as to provide more rapid and accurate diagnosis for the clinical practice.

In this work, we studied 769 CXR images from two hospitals during the same period. Therefore, the results have relatively high reliability. However, the dynamic range of image intensities in the two datasets was inconsistent, and proper image processing was necessary to simplify the implementation of deep learning. We then normalized the data to a range of −1024 to 1024 during preprocessing. Then, histogram equalization was carried out to further reduce the difference between the images and improve the generalization performance of the model. The resolution of the images was then further adjusted to 224×224 for network input. During the training process, data enhancement was performed, including random rotation (−15 to +15 degrees) and scaling (scaling factor between 0.5 and 1.5). These operations are standard in digital image processing and contributed to the data reproducibility of this work.

It is not enough to train the model and get results unless we understand what triggers the relevant output.

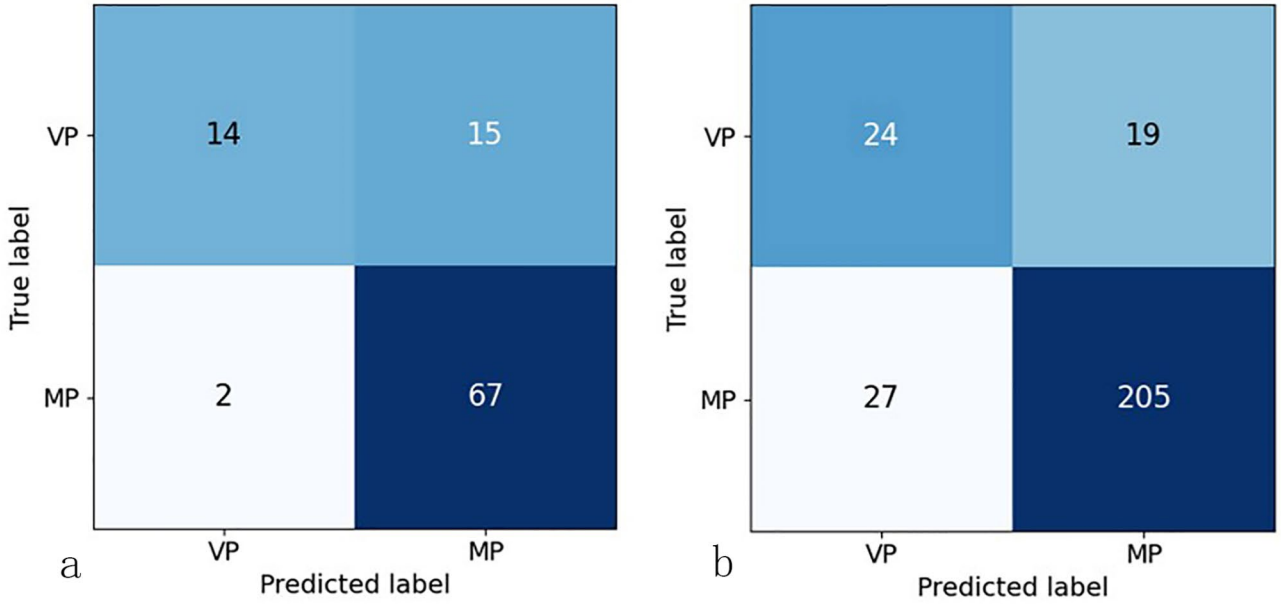

Fig. 4 The confusion matrices on the two test sets using the ResNet50 model pretrained on ZhangLabData

Table 2 Performance indices obtained by training with the ImageNet pre-training weights

	Number of Images		Resnet50	Densenet121	Efficientnetv2-s
validation	30VP/70 MP	Acc	80.00%	81.00%	82.00%
Test1	29VP/69MP	Acc	81.63%	75.51%	82.65%
		Auc	0.851	0.792	0.844
		Sen	0.884	0.928	0.957
		Spe	0.655	0.345	0.517
Test2	43VP/232MP	Acc	62.91%	74.55%	71.64%
		Auc	0.776	0.781	0.720
		Sen	0.595	0.733	0.754
		Spe	0.814	0.814	0.512

Acc: accuracy, Auc: Area Under the Curve, Sen: sensitivity, Spe: specificity

VP: viral pneumonia; MP: mycoplasma pneumonia

Table 3 Results of training ResNet50 using different data processing techniques (with pre-trained weights from ZhangLabData dataset)

HE	DA	Test1				Test2			
		Acc	Auc	Sen	Spe	Acc	Auc	Sen	Spe
×	×	76.53%	0.835	0.884	0.483	78.91%	0.541	0.935	0.000
✓	×	77.55%	0.812	0.913	0.448	74.91%	0.691	0.780	0.581
×	✓	77.55%	0.834	0.942	0.379	82.91%	0.693	0.953	0.163
✓	✓	82.65%	0.822	0.971	0.483	83.27%	0.758	0.884	0.558

HE: Histogram equalization

DA: Data augmentation

To deal with this black box, visualization techniques may help illustrate the basis of the model's predictions. In this study, CAM technology was used to present the model perception of identifying and classifying mycoplasma pneumonia samples from CXR images. As shown in Fig. 5, The sites that the model focused on basically matched the sites of disease that radiology experts would focus on in diagnosis.

In this study, we adopted three kinds of commonly used neural network architectures, namely the ResNet50, DenseNet121, and EfficientNetv2S, to classify CXR so as to determine the presence of mycoplasma pneumonia. We compared the performance of the different models. We found that the ResNet50, DenseNet121, and Effentnetv2-s models all showed relatively high accuracy, but the accuracy of the ResNet50 model was the most stable.

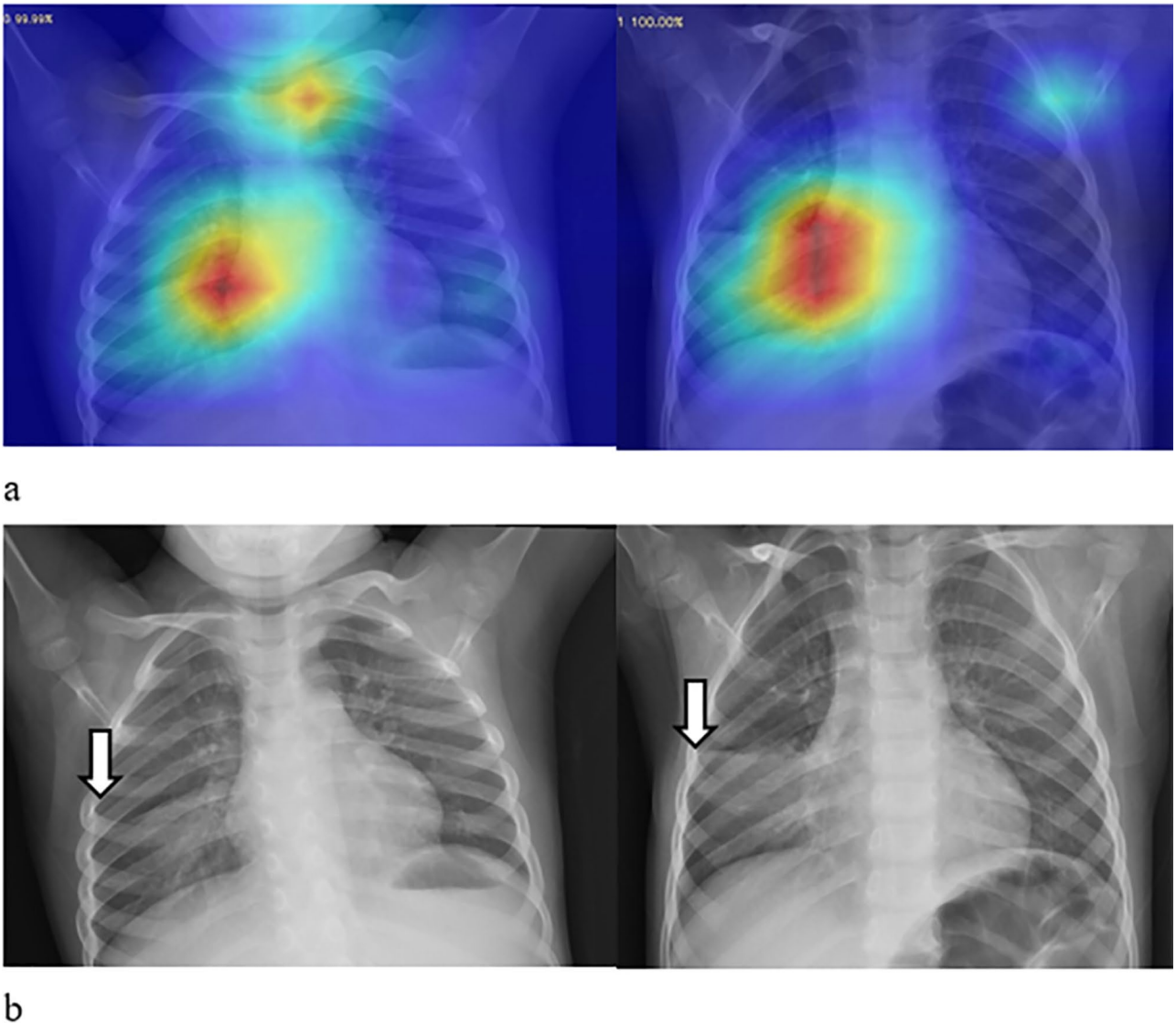

Fig. 5 The recognition of pathology areas by the model and human experts for sample pediatric chest radiographs in mycoplasma pneumonia. Respectively, (**a**) the original images with superimposed class activation maps to highlight the areas considered to be important in identifying the etiology by the model (**b**) the most clinically significant regions of pathology recognized by radiology experts (labeled by arrows). In (**a**), red regions correspond to high evidence for the pathogeny

The accuracy of 80.00% was achieved in the validation set (pretrained on ZhangLabData dataset). The model also showed robustness in two test sets, with accuracy of 82.65% and 83.27%, and AUC values of 0.822 and 0.758. The accuracy of the DenseNet121 and EfficientNetv2-S models in the validation set was similar with the ResNet50, but they perform worse in the test sets, showing inferior generalization ability. Overall, the ResNet50 model pretrained on ZhangLabData dataset showed the highest overall score in accuracy, sensitivity, and AUC, so it is the most suitable for the detection of mycoplasma pneumonia samples. This may be related to the structural characteristics of this model, whose main advantage is the addition of residual units, which can train very deep networks without the problem of disappearing or exploding gradients. This is consistent with the research results from Pablo et al. [22], who used different deep-learning models to analyze X-ray images to detect lung diseases. In addition, we found that the test results pretrained by the ZhangLabData dataset were better than the test results using ImageNet pre-training weights, which may be because the ZhangLabData dataset al.so contains the data of pediatric pneumonia, which is closer to the characteristics of the dataset in this paper [23]. The resulting model has better generalization performance.

Simultaneously, we compared several related studies that utilized deep learning methods in diagnosing pneumonia [13, 24–28] (see Table 4). Their results were a little

Table 4 Detection of different types of pneumonia using deep learning tools based on CXR

Reference	Data processing	Data augmentation	Type of pneumonia	Dataset	Result
[24]	Resizing	Flipping, cropping, zooming	Viral, bacterial	138 viral pneumonia and 262 bacterial pneumonia Chest X-Ray images	The models achieved an AUC of 0.919 ($P < 0.001$), with a sensitivity of 79.0% and specificity of 88.9%
[25]	Resizing, normalization	/	COVID-19,non-COVID-19 VP, BP	1493 non-COVID-19 viral pneumonia, 305 COVID-19 pneumonia and 2780 bacterial pneumonia Chest X-Ray images	The model achieved 97.4% ACC for COVID-19 vs. normal, 96.9% for COVID-19 Vs non-COVID-19 VP, 94.7% for COVID-19 vs. BP, and 90% for multi-class
[13]	Resizing, normalization	Shifting, zooming, flipping, rotation	Pneumonia and normal	1583 normal and 4273 pneumonia Chest X-Ray images	The Vgg16 network achieved 87% accuracy, 91% specificity and 91% pneumonia precision
[26]	Normalization, contrast limited adaptive histogram equalization (CLAHE)	Rescaling, rotation, shifting, shearing, zooming, flipping	Bacterial, coronavirus, normal	2780 bacterial pneumonia, 1724 coronavirus pneumonia and 1583 normal Chest X-Ray images	The Inception_Resnet_V2 network achieved 92.18% accuracy, 92.11% sensitivity, 96.06% specificity, 92.38% precision and 92.07 F1 score
[27]	/	/	COVID-19, non-COVID-19 VP, BP, normal	371 COVID-19 pneumonia, 4237 Non-COVID-19 viral pneumonia, 4078 bacterial pneumonia and 2882 normal Chest X-Ray images	The proposed model achieved 99.62% accuracy, 90.63% sensitivity, and99.89% specificity for COVID-19 vs. non-COVID-19 VP. For three-way classification, the model obtained 94.00% accuracy,91.30% sensitivity, and 84.78% specificity. For four-way classification, it achieved 93.42% accuracy,89.18% sensitivity, and98.92% specificity.
[28]	/	/	Bacterial, viral, and normal	2,538 bacterial pneumonia, 1,345 viral pneumonia and 1,349 normal Chest X-Ray images	The Inception V3 model achieved an accuracy of 92.8%, with a sensitivity of 93.2% and a specificity of 90.1% for pneumonia versus normal. It also attained an accuracy of 90.7%, with a sensitivity of 88.6% and a specificity of 90.9% for bacterial versus viral pneumonia.

better than that of the present study. Several factors may contribute to this finding. One possible reason is the different pneumonia pathogens examined; specifically, their studies predominantly focused on bacterial and/or viral pneumonia, whereas the CXR findings of mycoplasma pneumonia tend to be more diverse and atypical compared to those of bacterial pneumonia [29]. Another reason is the limited number of chest radiographs utilized in this study. Consequently, future efforts should aim to enlarge the sample size of CXR, also with image enhancement techniques, thereby enhancing the reliability of the proposed method. Furthermore, to bolster the learning performance of deep learning in diagnosing mycoplasma pneumonia, it is essential to incorporate clinical data, such as the age of children, onset of symptoms, fever, and other laboratory examination. We intend to integrate this type of information in our future study.

The present study has some limitations. First, the experimental model was based on the comparison between mycoplasma pneumonia and viral pneumonia, and the validity of the model may have been affected by the number and proportion of cases. In the future, multicenter study will be carried out, with larger-scale datasets that can better verify the generality of the deep learning models. Cross validation can also be applied to validate their performance. Second, some cases with mixed infection (both viral and mycoplasma) were encountered in data collection, and were excluded from the current dataset. Further study is needed to correctly identify these cases. Third, bacterial infections were not included in the present study. It is expected that three-way classifications (mycoplasma pneumonia/viral pneumonia/no pneumonia) or even four-way classifications (mycoplasma pneumonia/viral pneumonia/bacterial pneumonia/no pneumonia) will be carried out in our future work. Fourth, this study only focused on deep learning models for classification, as they can achieve automatic feature extraction, require fewer manual interventions and usually are more robust than traditional machine learning methods. In the future, more extensive comparisons can be performed with machine learning classifiers such as support vector machine (SVM), K nearest neighbors (KNN), and random forest based on radiomics features.

Conclusion

In this study, we used deep learning to classify CXR images for early diagnosis of mycoplasma pneumonia. The results showed that although different deep

convolutional network models had different performances, they all show good performance, and the ResNet50 model had the best performance. Therefore, the deep-learning model based on CXR established in this study showed great potential in the diagnosis of mycoplasma pneumonia, and had important clinical value for the rapid diagnosis and early medical intervention of mycoplasma pneumonia in children.

This may mean that in the near future, deep learning can contribute to earlier and more accurate diagnosis of childhood mycoplasma pneumonia, or even pneumonia caused by other pathogens, provide important help for early clinical treatment, and greatly improve the prognosis of children. In the future, such computer-aided diagnosis (CAD) techniques can be integrated into IoMT (Internet of Medical Things)-based artificial intelligence systems, and deep learning methods will penetrate deeper into more aspects of medicine and provide early and accurate diagnosis for more diseases.

Acknowledgements
We thank all the participants involved in this study.

Author contributions
Fei Shi, and Wan-liang Guo made substantial contributions to the design of this work. Xing-hao Lan, Yun-xu Zhang and Wei-hua Yuan contributed to the data collection and analysis. Xing-hao Lan, Fei Shi, and Wan-liang Guo interpreted the results to draft and revise the manuscript.

Funding
No financial or non-financial benefits have been received or will be accepted from any party related directly or indirectly to the subject of this article.

Data availability
The datasets used and/or analysed during the current study available from the corresponding author on reasonable request.

Declarations

Ethics approval and consent to participate
The pediatric pneumonia dataset was exempted from review by the institutional review board of the Children's Hospital of Soochow University and Changzhou Children's Hospital.

Consent for publication
Written informed consent was obtained from parents.

Competing interests
The authors declare no competing interests.

Author details
[1]Radiology department, Children's Hospital of Soochow University, Suzhou 215025, China
[2]School of Electronic and Information Engineering, Soochow University, Suzhou 215006, China
[3]Radiology department, Changzhou Children's Hospital of Nantong University, Changzhou 213000, China

Received: 29 February 2024 / Accepted: 2 November 2024
Published online: 11 November 2024

References

1. Wang YMS-M, Cho Y-H, et al. Clinical and epidemiological characteristics in children with community-acquired mycoplasma pneumonia in Taiwan: a nationwide surveillance. J Microbiol Immunol Infect. 2015;48(6):632–8. https://doi.org/10.1016/j.jmii.2014.08.003
2. Subspecialty Group of Respiratory Diseases, The Society of Pediatrics; Chinese Medical Association The Editorial Board. Chinese Journal of Pediatrics. Guidelines for management of community acquired pneumonia in children (the revised edition of 2013) (I). Zhonghua Er Ke Za Zhi. 2013;51:745–9. (in Chinese).
3. Tamura A, Matsubara K, Tanaka T, Nigami H, Yura K, Fukaya T. Methylprednisolone pulse therapy for refractory mycoplasma pneumoniae pneumonia in children. J Nfect. 2008;57:223–8.
4. Zhang Y, Zhou Y, Li S, Yang D, Wu X, Chen Z. The clinical characteristics and predictors of refractory mycoplasma pneumonia pneumonia in children. PLoS ONE. 2016;11:e0156465.
5. Wang Y, Xu D, Li S, Chen Z. Mycoplasma pneumoniae-associated necrotizing pneumonitis in children. Pediatr Int. 2012;54:293–7.
6. Lee HAE,Thomas, Hills et al. Respiratory syncytial virus: paying the immunity debt with interest. The Lancet Child & Adolescent Health. 2021;5(12):e44-e45. https://doi.org/10.1016/s2352-4642(21)00333-3
7. Kevin M. Richard F. Baker, Sang Woo Park et al. Preparing for uncertainty: endemic paediatric viral illnesses after COVID-19 pandemic disruption. The Lancet. 2022;400(10364):1663–1665. https://doi.org/10.1016/s0140-6736(22)01277-6
8. LeCun Y, Bengio Y, Hinton G. Deep learning. Nature. 2015;521(7553):436–44.
9. Calli E, Sogancioglu E, van Ginneken B, van Leeuwen KG, Murphy K. Deep learning for chest X-ray analysis: a survey. Med Image Anal. 2021;72. Article ID 102125.
10. Oliveira LL, Silva SA, Ribeiro LH, de Oliveira RM, Coelho CJ, AL SA. Computer-aided diagnosis in chest radiography for detection of childhood pneumonia. Int J Med Informatics. 2008;77(8):555–64.
11. Lakhani P, Sundaram B. Deep learning at chest radiography: automated classification of pulmonary tuberculosis by using convolutional neural networks. Radiology. 2017;284(2):574–82.
12. Prathiksha P. Pai, Sarika Hegde. Early detection of pneumonia using deep learning approach. Commun Comput Inform Sci. 2022;0(0):294–304. https://doi.org/10.1007/978-3-031-22485-0_27
13. Enes Ayan,Halil Murat Ünver. Diagnosis of pneumonia from chest X-ray images using deep learning. null. 2019;0(0):0–0. https://doi.org/10.1109/ebbt.2019.8741582
14. He K, Zhang X, Ren S, Sun J. Deep residual learning for image recognition, 2016 IEEE Conference on Computer Vision and Pattern Recognition (CVPR), 2016, pp. 770–778.
15. Huang G, Liu Z, Van Der Maaten L, Weinberger KQ, Recognition P. Densely connected convolutional networks, (CVPR), 2017, pp. 2261–2269.
16. Tan M, Le Q, Efficientnet. Rethinking model scaling for convolutional neural networks. International Conference on Machine Learning (ICML). 2019:6105–6114.
17. Daniel S, Kermany M, Goldbaum W, Cai, Carolina CS, Valentim H, Liang SL. Baxter identifying medical diagnoses and treatable diseases by image-based deep learning. Cell. 2018;172(5):1122–1131.e9.
18. Zhou B, Khosla A, Lapedriza A, Oliva A, Torralba A. Learning deep features for discriminative localization. 2016 IEEE Conference on Computer Vision and Pattern Recognition (CVPR), 2016, pp. 2921–2929.
19. Ken B, Waites,Deborah F, Talkington. Mycoplasma pneumoniaeand its role as a human pathogen. Clin Microbiol Rev. 2004;17(4):697–728. https://doi.org/10.1128/cmr.17.4.697-728.2004
20. Douglas IS. New diagnostic methods for pneumonia in the ICU. Curr Opin Infect Dis. 2016;29(2):1.
21. Jean-Louis V, David B, Nicolas L, et al. Rapid diagnosis of infection in the critically ill, a multicenter study of molecular detection in bloodstream infections, pneumonia, and sterile site infections. Crit Care Med. 2015;43(11):2283–91.
22. Pablo Vieira,Orrana LV, de Sousa et al. Deborah Magalhães. Detecting pulmonary diseases using deep features in X-ray images. Pattern Recognition. 2021;119(0):108081–108081.
23. Daniel Kermany MH, Goldbaum,Wenjia, Cai et al. Identifying Medical Diagnoses and Treatable Diseases by Image-Based Deep Learning. Cell. 2018;172(5):1122–1131.e9. https://doi.org/10.1016/j.cell.2018.02.010
24. Longjiang EB, Zhao,Hongsheng, Liu et al. Image-based deep learning in diagnosing the etiology of pneumonia on pediatric chest X-rays. Pediatric Pulmonology. 2021;56(5):1036–1044. https://doi.org/10.1002/ppul.25229

25. Tanvir Mahmud,Awsafur Rahman,Shaikh Anowarul Fattah. CovXNet: a multi-dilation convolutional neural network for automatic COVID-19 and other pneumonia detection from chest X-ray images with transferable multi-receptive feature optimization. Comput Biol Med. 2020;122(0):103869–103869. https://doi.org/10.1016/j.compbiomed.2020.103869
26. Khalid El Asnaoui,Chawki Youness. Using X-ray images and deep learning for automated detection of coronavirus disease. J Biomol Struct Dyn. 2020;39(10):3615–26. https://doi.org/10.1080/07391102.2020.1767212
27. Abdullahi Umar Ibrahim,Mehmet Ozsoz,Sertan Serte, et al. Pneumonia classification using deep learning from chest X-ray images during COVID-19. Cognitive Computation. 2021;0(0):0–0. https://doi.org/10.1007/s12559-020-09787-5
28. Daniel Kermany,Michael H, Goldbaum,Wenjia, Cai et al. Identifying medical diagnoses and treatable diseases by image-based deep learning. Cell. 2018;172(5):1122–1131.e9. https://doi.org/10.1016/j.cell.2018.02.010
29. Chengjin Gao,Caiting Chu,Lei Xu. Chest imaging characteristics of mycoplasma pneumoniae pneumonia in children. Radiol Infect Dis. 2022;9(2):58–58. https://doi.org/10.4103/rid.rid_3_22

Publisher's note

Springer Nature remains neutral with regard to jurisdictional claims in published maps and institutional affiliations.